Iranian Journal of Organic Chemistry Vol. 10, No. 1 (2018) 2291-2299

Structural and spectral study of MAG_3 molecule

Mehdi Nabati*

Synthesis and Molecular Simulation Laboratory, Chemistry Department, Pars Isotope Company, P.O. Box: 1437663181, Tehran, Iran

Received: November 2017; Revised: December 2017; January: 2018

Abstract: In the present study, the density functional theory (DFT-B3LYP) method with 6-31+G(d,p) basis set was used for optimizing and studying the electronic structural properties of (2-mercaptoacetyl)glycylglycylglycine or MAG_3 molecule as an API at 298.15 K temperature and 1 atmosphere pressure. These bond orders data showed that the lone pair electrons of nitrogen atoms have resonance with carbonyl groups. So, these nitrogen atoms cannot easily be used as donating sites to connecting with an electrophile group. And also, Natural Bond Orbital (NBO) population analysis and the molecular electrostatic potential (MEP) surface of the structures were studied by mentioned level of theory. These studies indicate the less local reactivity of nitrogen atoms. To better understand of the MAG_3 molecular structure, the spectral properties of molecule were studied.

Keywords: DFT study, MAG_3, Nuclear medicine, Radiopharmaceutical, Reactivity, Stability.

Introduction

Radioisotope renography is a form of medical imaging of the kidneys that uses radiolabelling. A renogram, which may also be known as a MAG_3 scan, allows a nuclear medicine physician or a radiologist to visualize the kidneys and learn more about how they are functioning. The two most common radiolabelled pharmaceutical agents used are Tc99m-MAG_3 (MAG_3 is also called mercaptoacetyltriglycine or mertiatide) and Tc99m-DTPA (diethylenetriaminepentacetate). Some other radiolabelled pharmaceuticals are EC (Ethylenedicysteine) and 131-iodine labeled OIH (ortho-iodohippurate). After injection the radiopharmaceutical medicine into the venous system, the compound is excreted by the kidneys and its progress through the renal system can be tracked with a gamma camera. A series of images are taken at regular intervals.

Processing then involves drawing a region of interest (ROI) around both kidneys, and a computer program produces a graph of radioactivity inside the kidney with time, representing the quantity of tracer, from the number of counts measured inside in each image (representing a different time point). If the kidney is not getting blood for example, it will not be viewed at all, even if it looks structurally normal in medical ultrasonography or magnetic resonance imaging. If the kidney is getting blood, but there is an obstruction inferior to the kidney in the bladder or ureters, the radioisotope will not pass beyond the level of the obstruction, whereas if there is a partial obstruction then there is a delayed transit time for the MAG_3 to pass. More information can be gathered by calculating time activity curves; with normal kidney perfusion, peak activity should be observed after 3–5 minutes. The relative quantitative information gives the differential function between each kidney's filtration activities [1-3].

*Corresponding author. Tel: +982188337023; Fax: +982188337024, E-mail: mnabati@ymail.com

MAG_3 is an acronym for mercaptoacetyltriglycine, a compound that is chelated with a radioactive element–technetium-99m. In 1986, MAG_3 was developed at the University of Utah by Dr. Alan R. Fritzberg, Dr. Sudhakar Kasina, and Dr. Dennis Eshima. The drug underwent clinical trials in 1987 and passed Phase III testing in 1988. ^{99m}Tc-MAG_3 has replaced the older iodine-131 orthoiodohippurate or I131-Hippuran because of better quality imaging regardless of the level of renal function, and with the benefit of being able to administer lower radiation dosages [4-6].
In the present research work, the theoretical studies are done on the MAG_3 nuclear medicine by density functional theory (DFT) computational method. In this way, we investigate and discuss the structural, stability, reactivity, and spectral properties and natural bond orbital (NBO) population analysis of the mentioned radiopharmaceutical. We hope that our findings can solve the complicated subjects for this radiopharmaceutical.

Results and discussion

Figure **1** indicates the structure of (2-mercaptoacetyl)glycylglycylglycine or MAG_3 compound.

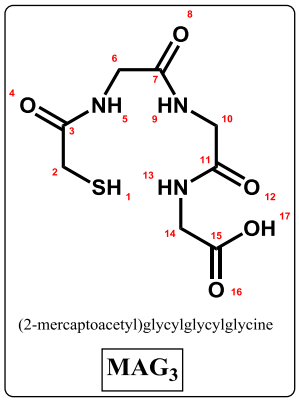

Scheme 1: The molecular structure of MAG_3 compound.

This molecular structure has been optimized by B3LYP/6-31+G(d,p) basis set of theory. The optimized geometry of the molecular structure is shown in Figure **2**. During the present study, the molecule is discussed from the point of views of structural, spectral and reactivity properties.

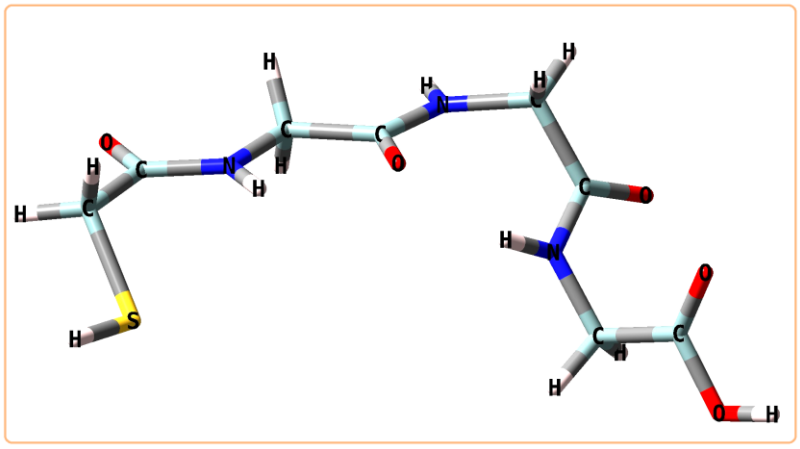

Figure 2: The optimized structure of MAG_3 compound.

Structural properties of MAG_3

Table **1** has collected the bond lengths, bond angles, dihedral angles and bond orders data of the MAG_3 compound. It can be seen from the data, the bond order (B.O.) of C3-N5, C7-N9 and C11-N13 bonds are 1.208, 1.064 and 1.048, respectively. These data shows that the lone pair electrons of nitrogen atoms have resonance with carbonyl groups. So, these nitrogen atoms cannot easily be used as donating sites to connecting with an electrophile group. In contrast, the B.O. of N-H bonds of the molecule is around 0.68, and it means that the hydrogen atoms of N-H bonds are acidic. Then, these N-H bonds are cleaved in alkaline pH and the nitrogen atoms can change to good nuclephile sites. Also, we can see the C-N-C bond angles are 119-122 degree. These bond angles are more than the usual pyramidal nitrogen bond angle (107 degree). It can be deduced that these nitrogen atoms have more angular freedom to bond composition with other molecules or chemical agents. From another

view, the S1-C2-C3-N5, N5-C6-C7-N9 and N9-C10-C11-N13 dihedral angles are 54, 178 and 63 degree, respectively. It can be concluded that the chelating atoms are not in good position for complex making with a radionuclide. So, this molecule can hardly compose a complex with an electrophile core.

Table 1: Bond lengths, bond angles, dihedral angles and bond orders data of the MAG_3 compound.

Bonds	Bond length (Å)	Bond Order (B.O.)	Bond angles	Angles (degree)
S1-H	1.351	0.962	S1-C2-C3	109.504
S1-C2	1.896	0.994	C2-C3-O4	122.385
C2-H	1.079	0.896	C2-C3-N5	115.248
C2-C3	1.515	0.980	N5-C3-O4	122.350
C3-O4	1.218	1.656	C3-N5-H	123.594
C3-N5	1.347	1.208	C3-N5-C6	120.060
N5-H	1.000	0.675	C6-N5-H	116.329
N5-C6	1.446	0.852	N5-C6-C7	107.902
C6-H	1.084	0.747	C6-C7-O8	121.729
C6-C7	1.518	0.881	C6-C7-N9	115.519
C7-O8	1.228	1.249	N9-C7-O8	122.752
C7-N9	1.342	1.064	C7-N9-H	120.351
N9-H	0.998	0.679	C7-N9-C10	121.743
N9-C10	1.467	0.779	C10-N9-H	117.905
C10-H	1.081	0.755	N9-C10-C11	112.529
C10-C11	1.525	0.860	C10-C11-O12	122.403
C11-O12	1.217	1.279	C10-C11-N13	114.217
C11-N13	1.352	1.048	C11-N13-H	119.270
N13-H	1.001	0.672	C11-N13-C14	119.548
N13-C14	1.440	0.858	C14-N13-H	120.518
C14-H	1.081	0.794	N13-C14-C15	111.102
C14-C15	1.508	0.887	C14-C15-O17	109.397
C15-O16	1.199	1.353	S1-C2-C3-N5	54.415
C15-O17	1.357	0.893	N5-C6-C7-N9	178.418
O17-H	0.968	0.580	N9-C10-C11-N13	63.336

The natural bond orbitals (NBOs) population analysis data of the molecular structure has been collected in Table **2**. It can be seen from the data that the nitrogen atoms use more s orbitals in composition of N-H bonds. These NBOs easily proves the acidic property the hydrogen atoms of the N-H bonds. Also, we can see that the nonbonding lone pair electrons of the N5 and N9 atoms show more s orbitals while the N13 atom participates less s orbital for its nonbonding electrons. This means that the N13 atom likes more to make resonance with carbonyl group than other nitrogen atoms, but the carboxylic acid group causes the less tendency of this atom for resonance with carbonyl group. So, it can be seen that the N-C=O possible resonance of N5 atom is more than others.

Reactivity prediction of MAG_3

Study and discussion of frontier molecular orbitals (FMOs) can give us more information about the reactivity and stability of an organic compound [7-9]. From the DFT computations, the energies -7.02 and -0.72 eV show the energy states of HOMO and LUMO orbitals, respectively. The low energy of HOMO orbital indicates the low tendency of molecule to react with an electrophile agent. The HOMO-LUMO energies gap is 6.3 eV. This high content of energy shows the high stability of MAG_3. Figure **3** has collected the graphs of HOMO and LUMO orbitals with their molecular electrostatic potential graphs. These graphs show the HOMO and LUMO orbitals focus more on sulfur and nitrogen atoms, respectively. Also, the MEP graph of HOMO indicates the sulfur atom has more free electrons to attack an electrophile agent. Figure **4** shows the density of states (DOS) graph of occupied and virtual orbitals of MAG_3 molecule. So, it can be deduced that the MAG3 is a stable molecule because of high DOS amount of virtual orbitals and high HOMO-LUMO energies gap. In the molecular electrostatic potential (MEP) graph of

MAG_3 compound, blue and red colors show the electron-poor and electron-rich segments, respectively.

Table 2: Natural bond orbitals (NBOs) analysis data of the MAG_3 compound.

Bonds	Occupancy	Population/Bond orbital/Hybrids
σ(S1-C2)	1.97989	47.87% S1 ($sp^{6.53}d^{0.04}$), 52.13% C2 ($sp^{4.30}$)
σ(S1-H)	1.99116	57.86% S1 ($sp^{5.39}d^{0.04}$), 42.14% H (s)
σ(C2-H)	1.97870	63.56% C2 ($sp^{2.75}$), 36.44% H (s)
σ(C2-C3)	1.98189	51.44% C2 ($sp^{2.73}$), 48.56% C3 ($sp^{1.83}$)
σ(C3-O4)	1.99392	35.33% C3 ($sp^{2.12}$), 64.67% O4 ($sp^{1.50}d^{0.01}$)
π(C3-O4)	1.98595	29.84% C3 ($sp^{99.99}d^{0.19}$), 70.16% O4 ($sp^{90.48}d^{0.30}$)
σ(C3-N5)	1.99049	37.35% C3 ($sp^{2.15}$), 62.65% N5 ($sp^{1.70}$)
σ(N5-H)	1.98373	73.92% N5 ($sp^{2.18}$), 26.08% H (s)
σ(N5-C6)	1.98614	60.87% N5 ($sp^{2.18}$), 39.13% C6 ($sp^{3.32}d^{0.01}$)
σ(C6-H)	1.96874	63.55% C6 ($sp^{2.84}$), 36.45% H (s)
σ(C6-C7)	1.97873	50.70% C6 ($sp^{3.03}$), 49.30% C7 ($sp^{1.81}$)
σ(C7-O8)	1.99356	35.22% C7 ($sp^{2.15}$), 64.78% O8 ($sp^{1.49}d^{0.01}$)
π(C7-O8)	1.98676	27.32% C7 ($sp^{99.99}d^{0.93}$), 72.68% O8 ($sp^{99.99}d^{1.21}$)
σ(C7-N9)	1.99089	37.80% C7 ($sp^{2.06}$), 62.20% N9 ($sp^{1.69}$)
σ(N9-H)	1.98450	72.46% N9 ($sp^{2.37}$), 27.54% H (s)
σ(N9-C10)	1.98345	62.44% N9 ($sp^{2.02}$), 37.56% C10 ($sp^{3.59}d^{0.01}$)
σ(C10-H)	1.98241	63.58% C10 ($sp^{2.83}$), 36.42% H (s)
σ(C10-C11)	1.97763	51.47% C10 ($sp^{2.83}$), 48.53% C11 ($sp^{1.87}$)
σ(C11-O12)	1.99462	35.31% C11 ($sp^{2.02}$), 64.69% O12 ($sp^{1.43}d^{0.01}$)
π(C11-O12)	1.98708	29.58% C11 ($sp^{99.99}d^{2.34}$), 70.42% O12 ($sp^{99.99}d^{6.06}$)
σ(C11-N13)	1.98951	37.52% C11 ($sp^{2.11}$), 62.48% N13 ($sp^{1.83}$)
σ(N13-H)	1.98358	73.94% N13 ($sp^{2.18}$), 26.06% H (s)
σ(N13-C14)	1.98582	61.06% N13 ($sp^{2.06}$), 38.94% C14 ($sp^{3.30}d^{0.01}$)
σ(C14-H)	1.96954	63.49% C14 ($sp^{2.87}$), 36.51% H (s)
σ(C14-C15)	1.97556	51.07% C14 ($sp^{3.04}$), 48.93% C15 ($sp^{1.60}$)
σ(C15-O16)	1.99725	34.47% C15 ($sp^{1.92}$), 65.53% O16 ($sp^{1.38}d^{0.01}$)
π(C15-O16)	1.99267	30.26% C15 ($sp^{99.99}d^{2.39}$), 69.74% O16 ($sp^{99.99}d^{4.19}$)
σ(C15-O17)	1.99581	31.48% C15 ($sp^{2.64}d^{0.01}$), 68.52% O17 ($sp^{1.92}$)
σ(C17-H)	1.98875	76.86% C17 ($sp^{3.16}$), 23.14% H (s)
LP_1(S1)	1.99321	S1 ($sp^{0.44}$)
LP_2(S1)	1.97987	S1 ($sp^{44.44}d^{0.02}$)
LP_1(N5)	1.69910	N5 (sp)
LP_1(N9)	1.68851	N9 (sp)
LP_1(N13)	1.69572	N13 ($sp^{99.99}d^{0.03}$)

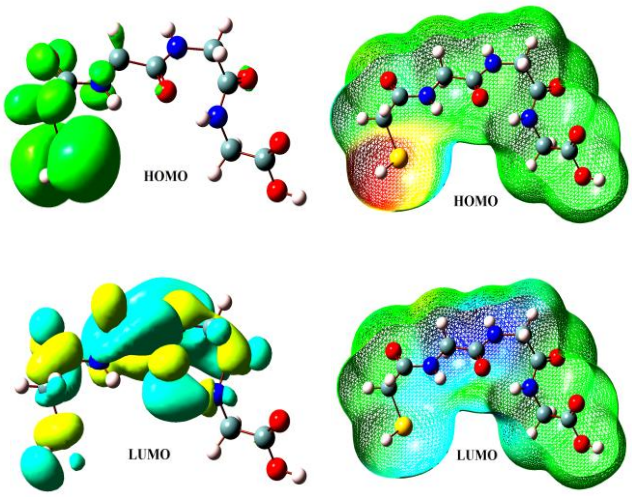

Figure 3: The frontier molecular orbitals of MAG_3 compound with their MEP graphs.

This graph indicates that sulfur and nitrogen atoms of molecule are electron-rich and electron-poor segments. It can be concluded from the MEP graph that the tendency of nitrogen atoms for bond making with a radionuclide is lower than the sulfur atom.

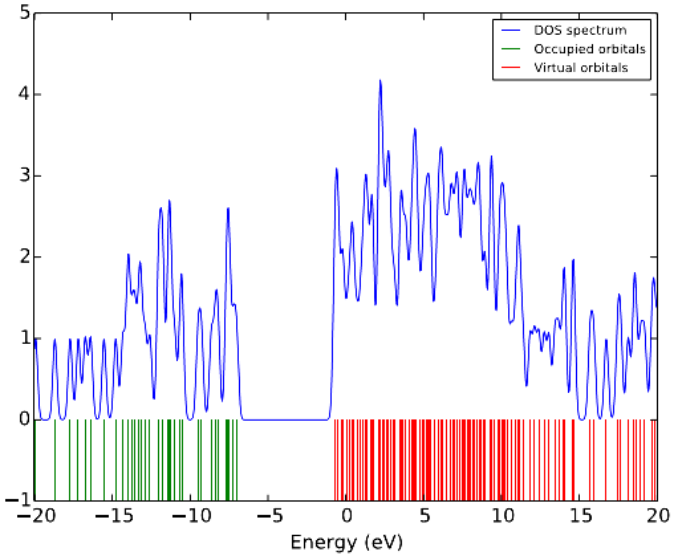

Figure 4: The density of states (DOS) graph of MAG_3 compound.

Spectral study of MAG$_3$

In chemistry, the identification of chemical molecules is done by spectroscopy methods [10-12]. Here, the UV-Vis, IR and NMR spectral properties of the [^{18}F]FDG nuclear medicine are investigated and discussed.

The UV-Vis spectrum of the studied molecule is indicated in Figure **6**. In the UV-Vis spectrum, the peak at wavelength 239.590 nm with energy 41738.67344 cm^{-1} is related to the (HOMO to LUMO+1 (62%) and HOMO to LUMO+3 (11%)) transition. The other transitions (HOMO-2 to LUMO (10%), HOMO-2 to LUMO+1 (19%), HOMO to LUMO (17%), HOMO to LUMO+2 (36%), HOMO-2 to LUMO+9 (2%), and HOMO to LUMO+3 (5%)) take place at wavelength 232.109 nm with energy 43083.20896 cm^{-1}. Also, the HOMO-1 to LUMO (31%), HOMO-1 to LUMO+1 (14%), HOMO-1 to LUMO+6 (25%), HOMO-4 to LUMO+6 (3%), HOMO-1 to LUMO+2 (3%), HOMO-1 to LUMO+3 (7%), and HOMO-1 to LUMO+5 (4%) transitions are shown at wavelength 229.119 nm with energy 43645.38128 cm^{-1}.

Figure **7** indicates the IR spectrum of the studied molecule. IR [Harmonic frequencies (cm^{-1}), intensities (KM/Mole)]: 32.0821 (0.4288), 56.2491 (22.9392), 77.3389 (16.1071), 158.2622 (7.6596), 176.3020 (11.5051), 200.9349 (5.9516), 207.1264 (6.7791), 246.8455 (12.0935), 264.4946 (55.3973), 289.7452 (3.1140), 307.6511 (6.8917), 329.3199 (8.1851), 374.7291 (74.7576), 399.1475 (45.0568), 450.3324 (34.0773), 457.9595 (24.3089), 482.9022 (65.4987), 501.5775 (75.4407), 562.1054 (2.4528), 566.2320 (37.5899), 573.9641 (66.0553), 615.2708 (16.4420), 639.4512 (27.6797), 649.7122 (4.0427), 697.7093 (2.3177), 730.3676 (3.9885), 795.1859 (1.1722), 848.9250 (3.0972), 860.4250 (3.1626), 881.5872 (4.3470), 888.9403 (6.0813), 911.0165 (6.6974), 989.8910 (1.0948), 1000.6777 (9.0493), 1024.2237 (20.4452), 1039.3697 (2.6612), 1060.4884 (1.2217), 1093.7154 (4.6835), 1124.0376 (304.2043), 1147.4260 (4.8201), 1177.4343 (1.4630), 1217.3107 (1.6541), 1223.9733 (28.1177), 1228.8259 (1.5008), 1244.7235 (16.3306), 1263.6134 (74.0807), 1267.5627 (29.6663), 1278.1977 (44.9759), 1308.7410 (2.3269), 1347.9022 (8.7315), 1373.8241 (7.7577), 1394.8067 (47.3077), 1428.2062 (22.3861), 1452.4759 (11.2063), 1453.7193 (21.8938), 1481.2455 (17.8251), 1537.8434 (609.1496), 1567.8489 (93.8508), 1573.2076 (237.4625), 1772.3145 (220.7636), 1811.3486 (296.5571), 1819.9940 (405.7911), 1896.5246

(271.7562), 2660.5971 (11.8505), 3155.9664 (26.5714), 3196.6903 (4.8532), 3199.1779 (14.3169), 3205.0210 (7.4614), 3216.2231 (5.5598), 3258.6956 (0.2902), 3287.7302 (2.3171), 3313.8480 (0.1370), 3722.5620 (216.6043), 3753.1042 (92.8078), 3791.0273 (50.0795), and 3808.7574 (81.7806).

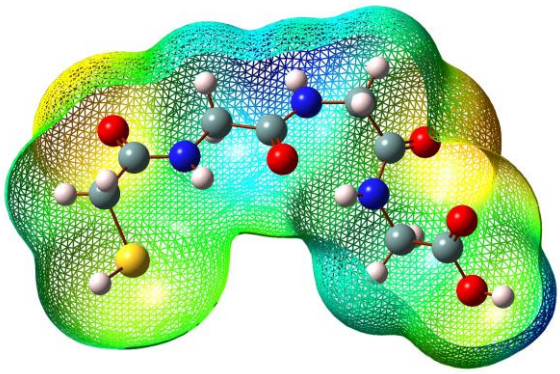

Figure 5: The molecular electrostatic potential (MEP) graph of MAG_3 compound.

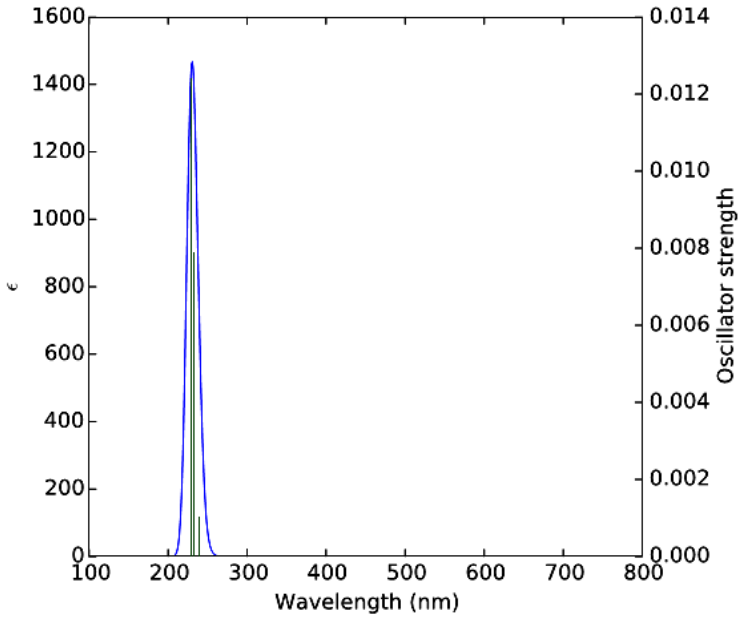

Figure 6: The UV-Vis spectrum of the MAG_3 compound.

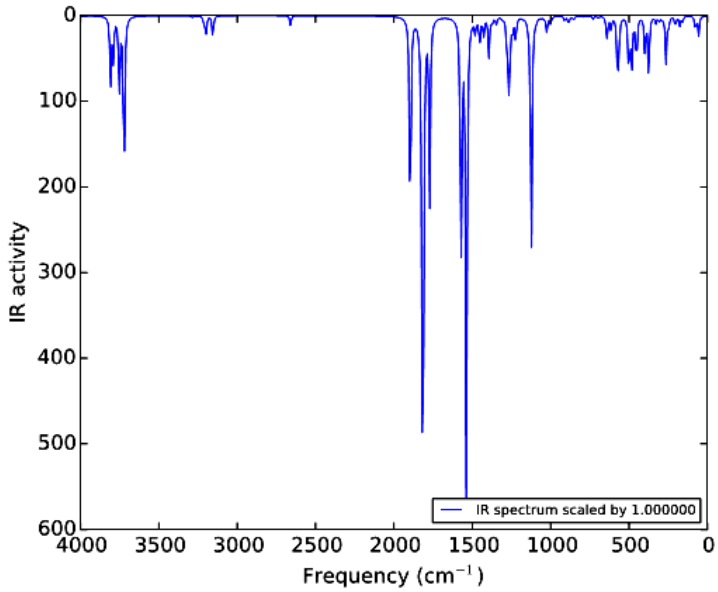

Figure 7: The IR spectrum of the MAG_3 compound.

The NMR technique is a good method for identification of the structure of the organic compounds [13]. The ^{1}H and ^{13}C chemical shifts of the MAG_3 compound are listed in Table **3**. The theoretical chemical shifts data is compared to the experimental values. The Figure **8** indicates the comparison between the theoretical and experimental ^{1}H and ^{13}C chemical shifts of the molecular structure at studied computational method. The large correlation coefficients show the accuracy of our computations. From the data of Table **3**, the protons connected to the nitrogen atoms are more de-shielded nucleus among all hydrogen atoms of MAG_3 structure, because the nitrogen atom has more electronegativity property. On other hand, the carbon atom of carbonyl groups is the de-shielded carbon atom. Also, we can see that the hydrogen atom of the S-H bond has appeared at chemical shift 2. This difference happens because of the proton exchange by O-H functional groups. These data indicate that our calculations are consistent with empirical data.

Computational method

In present research work, all computations were performed by Gaussian 03 package [14] using density functional theory (DFT) computational method by B3LYP functional with 6-31+G(d,p) basis set. The computations were done in the gas phase at room temperature. There were eight imaginary frequencies in IR computation for molecular structure. It proves accuracy of our computations.

Conclusions

During the present study, the structural and spectral (UV-Vis, IR and NMR) properties and reactivity of (2-mercaptoacetyl)glycylglycylglycine or MAG_3 compound are discussed. All discussions and investigations have done based on theoretical studies. From the computations, it was understood that MAG_3 is a more stable compound that its nitrogen atoms have resonance with carbonyl groups. So, they have fewer tendencies to react with an electrophile agent.

Acknowledgments

The corresponding author is grateful to Doctor Hojjatollah Salehi and Mr. Hossein Abbasi for providing valuable suggestions.

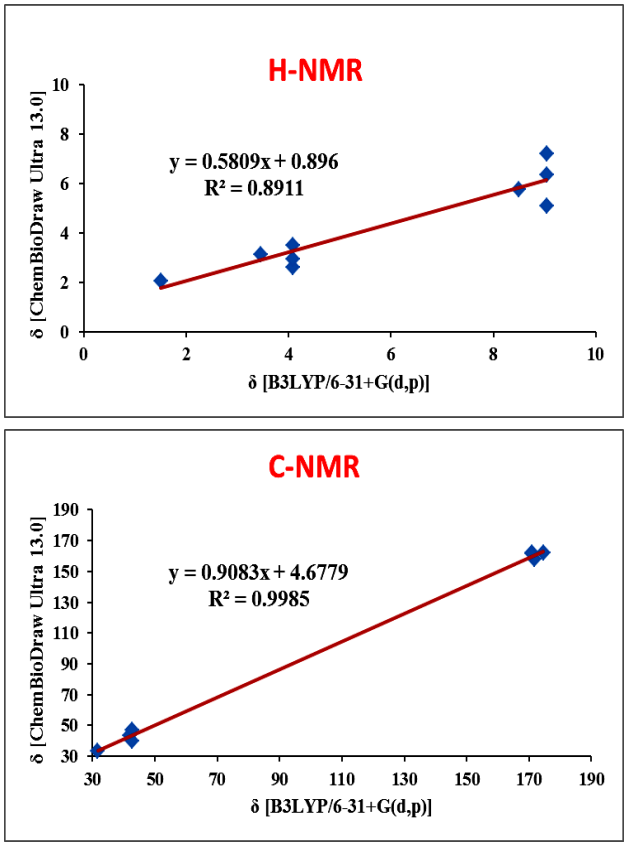

Figure 8: The relationship between theoretical and experimental NMR chemical shifts of the MAG_3 compound.

Table 3: The ^{1}H and ^{13}C chemical shifts of the MAG_3 compound.

Nucleus	Chemical Shift (ppm)	
	Theoretical chemical shifts ($\delta = \delta_{TMS} - \delta'$)	δ (Chemical shifts from ChemBioDraw Ultra 13.0)
H-1	2.066	1.500
H-2	3.128	3.460
H-5	6.377	9.040
H-6	3.517	4.090
H-9	5.106	9.040
H-10	2.632	4.090
H-13	7.199	9.040
H-14	2.968	4.090
H-17	5.771	8.500
C-2	33.310	31.700
C-3	157.899	171.700
C-6	43.378	42.000
C-7	162.268	171.000
C-10	46.824	42.800
C-11	161.748	171.000
C-14	39.670	42.600
C-15	161.989	174.600

References

[1] Ayaz, S. *J. Clin. Anal. Med.*, **2017**, *8*, 14.
[2] Erfani, M.; TShafiei, M. *Nucl. Med. Biol.*, **2014**, *30*, 317.
[3] Erfani, M.; TShafiei, M.; Charkhlooie, G.; Goudarzi, M. *Iran J. Nucl. Med.*, **2015**, *23*, 15.
[4] Fischer, S.; Hiller, A.; Smits, R.; Hoepping, A.; Funke, U.; Wenzel, B.; Cumming, P.; Sabri, O.; Steinbach, J.; Brust, P. *Appl. Radiat. Isot.*, **2013**, *74*, 128.
[5] Nabati, M. *J. Phys. Theor. Chem. IAU Iran*, **2016**, *13*, 133.
[6] Nabati, M.; Mahkam, M. *J. Phys. Theor. Chem. IAU Iran*, **2015**, *12*, 33.
[7] Nabati, M.; Mahkam, M. *Silicon*, **2016**, *8*, 461.
[8] Nabati, M.; Mahkam, M. *J. Phys. Theor. Chem. IAU Iran*, **2015**, *12*, 121.
[9] Nabati, M.; Mahkam, M.; Atani, Y. G. *J. Phys. Theor. Chem. IAU Iran*, **2016**, *13*, 35.
[10] Nabati, M.; Mahkam, M. *Org. Chem. Res.*, **2016**, *2*, 70.
[11] Nabati, M. *Chem. Method.*, **2017**, *2*, 128.
[12] Nabati, M.; Mahkam, M. *Inorg. Chem. Res.*, **2016**, *1*, 131.
[13] Nabati, M. *J. Phys. Theor. Chem. IAU Iran*, **2015**, *12*, 325.
[14] Frisch, M. J.; Trucks, G. W.; Schlegel, H. B.; Scuseria, G. E.; Robb, M. A.; Cheeseman, J. R.; Montgomery Jr., J. A.; Vreven, T.; Kudin, K. N.; Burant, J. C.; Millam, J. M.; Iyengar, S. S.; Tomasi, J.; Barone, V.; Mennucci, B.; Cossi, M.; Scalmani, G.; Rega, N.; Petersson, G. A.; Nakatsuji, H.; Hada, M.; Ehara, M.; Toyota, K.; Fukuda, R.; Hasegawa, J.; Ishida, M.; Nakajima, T.; Honda, Y.; Kitao, O.; Nakai, H.; Klene, M.; Li, X.; Knox, J. E.; Hratchian, H. P.; Cross, J. B.; Adamo, C.; Jaramillo, J.; Gomperts, R.; Stratmann, R. E.; Yazyev, O.; Austin, A. J.; Cammi, R.; Pomelli, C.; Ochterski, J. W.; Ayala, P. Y.; Morokuma, K.; Voth, G. A.; Salvador, P.; Dannenberg, J. J.; Zakrzewski, V. G.; Dapprich, S.; Daniels, A. D.; Strain, M. C.; Farkas, O.; Malick, D. K.; Rabuck, A. D.; Raghavachari, K.; Foresman, J. B.; Ortiz, J. V.; Cui, Q.; Baboul, A. G.; Clifford, S.; Cioslowski, J.; Stefanov, B. B.; Liu, G.; Liashenko, A; Piskorz, P.; Komaromi, I.; Martin, R. L.; Fox, D. J.; Keith, T.; Al- Laham, M. A.; Peng, C. Y.; Nanayakkara, A.; Challacombe, M.; Gill, P. M. W.; Johnson, B.; Chen, W.; Wong, M. W.; Gonzalez, C.; Pople, J. A. *Gaussian 03. Revision B.01*. Gaussian Inc. Wallingford. CT. **2004**.